Acta Pharmaceutica Sinica B 2018;8(3):409–419

Chinese Pharmaceutical Association
Institute of Materia Medica, Chinese Academy of Medical Sciences

Acta Pharmaceutica Sinica B

www.elsevier.com/locate/apsb
www.sciencedirect.com

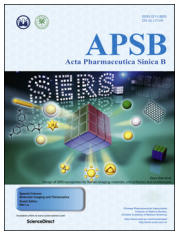

ORIGINAL ARTICLE

C_{19}-Diterpenoid alkaloid arabinosides from an aqueous extract of the lateral root of *Aconitum carmichaelii* and their analgesic activities

Qinglan Guo[†], Huan Xia[†], Xianhua Meng, Gaona Shi, Chengbo Xu, Chenggen Zhu, Tiantai Zhang[*], Jiangong Shi[*]

State Key Laboratory of Bioactive Substance and Function of Natural Medicines, Institute of Materia Medica, Chinese Academy of Medical Sciences and Peking Union Medical College, Beijing 100050, China

Received 31 January 2018; received in revised form 1 March 2018; accepted 18 March 2018

KEY WORDS

Ranunculaceae;
Aconitum carmichaelii;
C_{19}-diterpenoid alkaloid;
Arabinoside;
Aconicarmichosides E–L;
Analgesic effect;
Structure–activity relationship

Abstract Eight new C_{19}-diterpenoid alkaloid arabinosides, named aconicarmichosides E–L (**1**–**8**), were isolated from an aqueous extract of the lateral roots of *Aconitum carmichaelii* (Fu Zi). Their structures were determined by spectroscopic and chemical methods including 2D NMR experiments and acid hydrolysis. Compounds **1**–**8**, together with the previously reported four neoline 14-*O*-arabinosides from the same plant, represent the only examples of glycosidic diterpenoid alkaloids so far. At a dose of 1.0 mg/kg (i.p.), as compared with the black control, compounds **1**, **2**, and **4**–**6** exhibited analgesic effects with $>65.6\%$ inhibitions against acetic acid-induced writhing of mice. Structure–activity relationship was also discussed.

*Corresponding authors.
E-mail addresses: ttzhang@imm.ac.cn (Tiantai Zhang), shijg@imm.ac.cn (Jiangong Shi).
†These authors made equal contribution to this work.

Peer review under responsibility of Institute of Materia Medica, Chinese Academy of Medical Sciences and Chinese Pharmaceutical Association.

https://doi.org/10.1016/j.apsb.2018.03.009

1. Introduction

The lateral and principle roots of the poisonous plant *Aconitum carmichaelii* Debx. (Ranunculaceae), named "Fu Zi" and "Wu Tou" in Chinese, respectively, are important traditional Chinese medicines used for the treatment of rheumatalgia, neuralgia, arrhythmia, acardianeuria, and inflammations[1–4]. Considerable chemical and pharmacological studies have previously been reported, along with isolation of more than a hundred compounds from various extracts of different parts of *A. carmichaelii*[2–12]. Among the reported chemical constituents, diterpenoid alkaloids were recognized as active components, especially the lipophilic diesterified aconitane-type C_{19}-diterpenoid alkaloids were identified as the main toxic constituents. In addition, the previous reports showed that toxicity of these medicines was dramatically reduced by processing and decocting because contents of the toxic diesterified aconitane-type alkaloids were remarkably decreased by the treatments[13–16]. However, in the chemical studies, organic solvents, such as benzene, chloroform, methanol, and ethanol, were applied for extracting the raw and processed plant materials[2–11]. The extraction procedures also differ from a classic protocol of utilization by decocting the medicines with water. Therefore, as part of our program to systematically study the chemical diversity of traditional Chinese medicines and their biological effects[17–42], an aqueous decoction of the raw lateral roots of *A. carmichaelii* was investigated. In previous papers, we reported four new hetisan-type, three new napeline-type, a new arcutine-type, and a novel type C_{20}-diterpenoid alkaloids, twenty-six new aconitane-type C_{19}-diterpenoid alkaloids including four unique glycosidic neoline derivatives with isomeric arabinosyls, two new 2-(quinonylcarboxamino)benzoates, and seven new aromatic acid derivatives, as well as solvent-/base-/acid-dependent transformation and equilibration between alcohol iminium and aza acetal forms of the napeline-type C_{20}-diterpenoid alkaloids[43–49]. This paper describes isolation and structural characterization of eight aconitane-type C_{19}-diterpenoid alkaloid L-arabinosides (**1**–**8**, Fig. 1) as well as their analgesic activities from the same decoction.

2. Results and discussion

Compound **1** was isolated as a colorless gum with $[\alpha]_D^{20}$ +25.5 (*c* 0.20, MeOH). The IR spectrum of **1** showed a strong absorption band (3365 cm^{-1}) due to hydroxyl groups. The (+)-HR-ESI-MS and NMR spectroscopic data (Experimental Section 4.3.1, and Tables 1 and 2) indicated that **1** had the molecular formula $C_{29}H_{47}NO_{10}$. The ^{1}H NMR spectrum of **1** in CD_3OD showed resonances characteristic for an aconitane-type C_{19}-diterpenoid alkaloid, including an *N*-CH_2CH_3 unit at δ_H 3.30 and 3.25 (1H each, m, H_2-20) and 1.43 (3H, t, J = 7.5 Hz, H_3-21) and three methoxy groups at δ_H 3.40 (s, OMe-16), 3.35 (s, OMe-6), and 3.32 (s, OMe-18); four oxymethines at δ_H 4.33 (brd, J = 7.0 Hz, H-6), 4.19 (brs, H-1), 4.14 (dd, J = 5.0 and 4.5 Hz, H-14), and 3.35 (m, H-16); one nitrogen-bearing methine at δ_H 3.27 (brs, H-17); an oxymethylene at δ_H 3.57 and 3.50 (1H each, d, J = 8.0 Hz, H_2-18); and a nitrogen-bearing methylene at δ_H 3.39 and 3.06 (1H each, d, J = 12.5 Hz, H_2-19); as well as partially overlapped resonances due to four aliphatic methylenes (H_2-2, H_2-3, H_2-12, and H_2-15) and five aliphatic methines (H-5, H-7, H-9, H-10, and H-13) between δ_H 1.50 and 2.42. Additionally the spectrum showed signals diagnostic for a pentose moiety, consisting of four oxygen-bearing methines at δ_H 5.11 (d, J = 5.5 Hz, H-1′), 4.16 (dd, J = 8.0 and 5.5 Hz, H-2′), 4.02 (dd, J = 8.0 and 7.0 Hz, H-3′), and 3.76 (m, H-4′), and an oxygen-bearing methylene at δ_H 3.75 (m, H-5′a) and 3.65 (dd, J = 12.5 and 6.5 Hz, H-5′b). The ^{13}C NMR and DEPT spectra showed 29 carbon signals corresponding to the above units and three quaternary carbons including an oxygen-bearing carbon at δ_C 74.6 (C-8). Comparison of the spectroscopic data with those of aconicarmichosides A–D[48] indicated that **1** was an isomer of neoline β-L-arabinofuranoside. Specifically compared with the NMR spectroscopic data of aconicarmichoside D[48], the resonances of H-1, H-2a, H-5, and H-16 and C-1, C-1′, and C-17 in **1** were remarkably deshielded by $\Delta\delta_H$ +0.19, +0.38, +0.05, and +0.05 and $\Delta\delta_C$ +5.2, –5.9, and +2.0, respectively, whereas H-2b, H-3b, H-9, and H-13 and C-2 and C-14 were shielded by $\Delta\delta_H$ –0.09, –0.26, –0.15, and –0.14 and $\Delta\delta_C$ –6.3 and –6.6. These differences suggested that location of the hydroxyl and arabinosyloxy at C-1 and C-14 in aconicarmichoside D was exchanged in **1**, which was proved by 2D NMR data analysis as below.

The proton and corresponding hydrogen-bearing carbon resonances in the NMR spectra of **1** were unambiguously assigned (Table 1) by analysis of the HSQC spectroscopic data. In the ^{1}H–^{1}H COSY spectrum of **1**, homonuclear vicinal coupling correlations of H-1/H_2-2/H_2-3, H-5/H-6/H-7, H-14/H-9/H-10/H_2-12/H-13/H-14, H_2-15/H-16, and H_2-20/H_3-21 demonstrated the presence of five spin systems separated by the quaternary carbons and/or heteroatoms in the aglycone moiety (Fig. 2, thick lines). The HMBC spectrum showed two- and three-bond correlations (Fig. 2, red arrows) from H_2-3 to C-4; from H-5 to C-4, C-18, and C-19; from H_2-18 to C-3, C-4, C-5, and C-19; and from H_2-19 to C-3, C-4, and C-5, indicating that the quaternary C-4 connected to C-3, C-5, C-18, and C-19. The HMBC correlations from H-7 to C-8, C-9, and C-15 and from H-9 to C-7, C-8, and C-15, together with their chemical shifts, revealed that the oxygen-bearing quaternary C-8 was linked by C-7, C-9 and C-15. The HMBC correlations from H-1 to C-3, C-10, and C-11; from H-5 to C-10, C-11, and C-17; from H-10 to C-1, C-5, C-11, and C-17; and from H-17 to C-5, C-6, C-10, and C-11 revealed a linkage of the quaternary C-11 with C-1, C-5, C-10 and C-17. The connection between C-13 and C-16 was confirmed by the HMBC correlations from H_2-12 to C-14 and C-16, from H-13 to C-15, from H-14 to C-16, and from H-16 to C-12 and C-14, though the vicinal coupling correlation between H-16 with H-13 and H_2-15 were undistinguishable in the ^{1}H–^{1}H COSY spectrum due to an overlap of the H-13 and H_2-15 resonances. In addition, the HMBC correlations from H-6 to C-17; from H-17 to C-6, C-8, C-19, and C-20; from H_2-19 to C-17 and C-20; from H_2-20 to C-17 and C-19; together their chemical shifts, demonstrated that C-17 connected with C-7 and *via* the nitrogen atom to both C-19 and C-20. The HMBC correlations from OCH_3-6 to C-6, from OCH_3-16 to C-16, and from OCH_3-18 to C-18 located the three methoxy groups at the corresponding carbons. In addition, the ^{1}H–^{1}H COSY cross-peaks of H-1′/H-2′/H-3′/H-4′/H_2–5′ and the HMBC correlations from H-1′ to C-1, C-3′, and C-4′ and from H-4′ to C-1′ proved that there was an arabinofuranosyloxy at C-1 of **1**. The coupling constant values of $J_{1',2'}$ (5.5 Hz), $J_{2',3'}$ (8.0 Hz), and $J_{3',4'}$ (7.0 Hz) confirmed the β-configuration of the arabinofuranosyloxy[48]. The hydroxyl group must be located at C-8 according to the chemical shift of this carbon and the molecular formula requirement of **1**. Thus, the planar structure of **1** was proved as shown. In the ROESY spectrum of **1**, the correlations between H-1 with H-10 and H-12a, between H-3a and H_2-18, between H-5 with H-10 and H_2-18, between H-6 and H-9, between H-10 with H-12a and H-14, and between H-14 with H-9 and H-13 demonstrated that

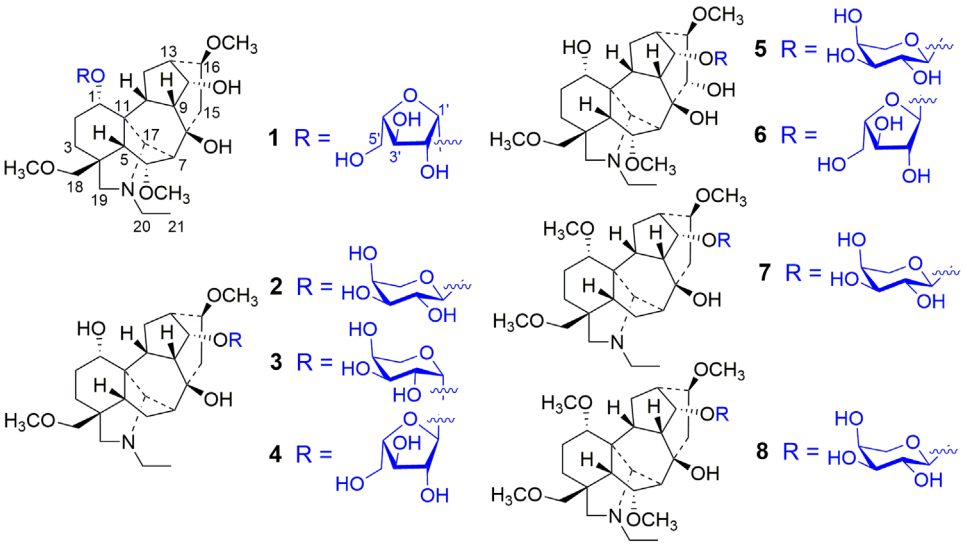

Figure 1 The structures of compounds **1**–**8**.

these hydrogens were oriented on the same side of the ring system. Meanwhile, the ROESY correlations between H-3b with H-19b, between H-16 and H-12b, and between H-17 with H-12b and H_3-21 revealed that these hydrogens were oriented on the other side of the ring system. Additionally, the NOE correlations between H-1′ with H-1 and H-2a further supported location of the sugar unit at C-1. Comparing with those of aconicarmichosides A–D from the same extract[48], the specific rotation of **1** suggested that the aglycone and sugar moieties in these compounds had the same absolute configurations. Thus, the structure of compound **1** is determined as neoline 1-*O*-*β*-L-arabinofuranoside, and named aconicarmichoside E.

Compound **2**, a colorless gum with $[\alpha]_D^{20}$ –24.8 (*c* 0.63, MeOH), has the molecular formula $C_{28}H_{45}NO_9$ as determined by (+)-HR-ESI-MS and NMR spectroscopic data (Experimental Section 4.3.2, and Tables 1 and 2). Comparison of the NMR spectroscopic data of **2** and **1** demonstrated that **2** had one less methoxy group than **1**. Especially the chemical shifts of proton and carbon resonances for the pentose moiety in the two compounds were completely different. This suggests that **2** is a demethoxy analogue of **1** with simultaneous change in the sugar moiety. Subsequent analysis of 2D NMR spectroscopic data (Figs. 2 and 3) confirmed that the aglycone of **2** was 6-demethoxyneoline (isotalatizidine). Particularly the ^{1}H–^{1}H COSY cross-peaks of H-1′/H-2′/H_2-3′/H-4′/H_2-5′ and the HMBC correlations from H-1′ to C-5′ and from H_2-5′ to C-1′, together with the coupling constant values of $J_{1',2'}$ (6.6 Hz) and $J_{3',4'}$ (3.6 Hz), verified that the pentosyl in **2** was *α*-arabinopyranosyl[48]. Meanwhile, the HMBC correlations from H-1′ to C-14 and from H-14 to C-1′ located the *α*-arabinopyranosyl at C-14 in **2**. Furthermore, from the acid hydrolysis of **2**, isotalatizidine {$[\alpha]_D^{20}$ +23.4 (*c* 0.09, MeOH)} and L-arabinose {$[\alpha]_D^{20}$+106.3 (*c* 0.10, H_2O)} were isolated and identified by comparison of the ^{1}H NMR spectroscopic data and the specific rotation value with those of the authentic samples {isotalatizidine, $[\alpha]_D^{20}$+18.4 (*c* 0.04, MeOH); L-arabinose, $[\alpha]_D^{20}$+113.3 (*c* 0.29, H_2O)[48]}. Therefore, the structure of compound **2** was determined as isotalatizidine 14-*O*-*α*-L-arabinopyranoside and named aconicarmichoside F.

Compound **3**, a colorless gum with $[\alpha]_D^{20}$ +28.3 (*c* 0.14, MeOH), showed spectroscopic data similar to those of **2** (Experimental Section 4.3.3 and Tables 1 and 2), except that the H-9 and H-14 and C-13 resonances in **3** were significantly shielded by $\Delta\delta_H$ −0.13 and −0.09 and $\Delta\delta_C$ −2.1, respectively, whereas H-13 and C-9 were deshielded by $\Delta\delta_H$+0.09 and $\Delta\delta_C$ +2.0. Especially the anomeric hydrogen and carbon resonances were changed significantly from δ_H 4.36 (d, J = 6.6 Hz) and δ_C 103.1 in **2** to δ_H 4.95 (d, J = 3.0 Hz) and δ_C 100.3, while the NMR data of arabinosyl in **3** were in good agreement with those of *β*-arabinopyranosyl in neoline 14-*O*-*β*-L-arabinopyranoside (aconicarmichoside B) isolated from the same extract[48]. This indicates that **3** is an isomer of **2** with replacement of *α*-L-arabinopyranosyl by *β*-L-arabinopyranosyl. The deduction was further confirmed by 2D NMR spectroscopic data of **3** (Figs. 2 and 3) as well as by isolation and identification of isotalatizidine and L-arabinose from the acid hydrolysate of **3**. Therefore, the structure of compound **3** was determined as isotalatizidine 14-*O*-*β*-L-arabinopyranoside and named aconicarmichoside G.

Compound **4** was obtained as a colorless gum with $[\alpha]_D^{20}$ –43.7 (*c* 0.40, MeOH). The spectroscopic data of **4** indicate that it is another isomer of **2** and **3** differing only in the arabinosyl moiety. The NMR spectroscopic data showed that the anomeric hydrogen and carbon of arabinosyl had more deshielded chemical shifts at δ_H 5.05 (H-1′) and δ_C 109.2 (C-1′) than those in **2** and **3**. Meanwhile, the H-1′ resonance of **4** appeared as a broad singlet instead of the doublets of **2** and **3**. In particular the chemical shifts and coupling pattern of the arabinosyl moiety in **4** were well consistent with those of *α*-arabinofuranosyl in aconicarmichoside C (neoline 14-*O*-*α*-L-arabinofuranoside)[48], indicating that an *α*-L-arabinofuranosyl in **4** replaced the L-arabinopyranosyls in **2** and **3**. This was verified by the ^{1}H–^{1}H COSY cross-peaks of H-1′/H-2′/H-3′/H-4′/H_2-5′ and the HMBC correlations from H-1′ to C-4′ and from H-4′ to C-1′ (Fig. 2). In addition, the HMBC correlations from H-1′ to C-14 and from H-14 to C-1′ confirmed location of the sugar unit in **4**. Therefore, the structure of compound **4** was determined and named aconicarmichoside H.

Compound **5**, a colorless gum with $[\alpha]_D^{20}$ –7.7 (*c* 0.15, MeOH), has the molecular formula $C_{29}H_{47}NO_{11}$ as determined by (+)-HR-ESI-MS combined with NMR spectroscopic data. Comparison of the NMR spectroscopic data of **5** and **1** (Tables 1 and 2) demonstrated that the methylene (CH_2-15) of the aglycone in **1**

Table 1 The ^{1}H NMR spectroscopic data (δ) for compounds **1**–**8**[a].

No.	**1**	**2**	**3**	**4**	**5**	**6**	**7**	**8**
1	4.19 brs	4.05 brs	4.06 brs	4.06 brs	3.94 brs	3.99 brs	3.57 brs	3.52 brs
2a	2.00 m	1.68 m	1.68 m	1.68 m	1.58 m	1.62 m	1.93 m	1.91 m
2b	1.51 m	1.62 m	1.62 m	1.62 m	1.55 m	1.59 m	1.44 m	1.38 m
3a	2.02 m	1.93 m	1.93 dd (15.0, 5.0)	1.94 m	1.97 m	2.02 dd (14.4, 6.0)	1.88 dd (15.0, 4.8)	1.96 dd (15.0, 4.8)
3b	1.55 dt (15.5, 4.0)	1.81 m	1.82 dt (5.4, 15.0)	1.83 dt (15.0, 6.0)	1.77 dt (15.0, 6.0)	1.82 dt (6.0, 14.4)	1.60 dt (4.8, 15.0)	1.58 dt (4.8, 15.0)
5	2.42 d (7.0)	2.05 m	2.07 m	2.05 m	2.29 d (7.5)	2.35 d (6.6)	2.04 brs	2.35 d (6.6)
6a	4.33 brd (7.0)	2.10 m	2.08 m	2.07 m	4.26 brd (7.5)	4.23 brd (6.6)	2.05 m	4.29 brd (6.6)
6b		1.84 m	1.84 m	1.85 m			1.77 dd (15.0, 7.8)	
7	2.20 brs	2.24 brd (8.4)	2.28 brd (8.4)	2.25 brd (8.4)	2.44 brs	2.50 brs	2.19 brd (7.8)	2.11 brs
9	2.14 dd (6.5, 5.0)	2.40 dd (5.4, 4.8)	2.27 dd (6.0, 4.8)	2.29 dd (4.8, 6.0)	2.34 dd (5.5, 4.5)	2.27 dd (6.0, 4.8)	2.36 t (5.4)	2.34 dd (6.6, 4.8)
10	2.18 m	2.14 m	2.16 m	2.15 m	2.09 m	2.15 m	2.12 m	2.13 m
12a	2.10 m	2.14 m	2.14 m	2.15 m	2.10 m	2.15 m	2.11 m	2.12 m
12b	1.66 dd (14.5, 4.5)	1.47 m	1.50 dd (13.8, 4.2)	1.46 m	1.53 m	1.58 m	1.24 m	1.24 m
13	2.25 m	2.35 dd (6.6, 4.8)	2.44 dd (7.2, 4.8)	2.37 dd (6.6, 4.8)	2.31 dd (6.0, 4.5)	2.39 dd (6.6, 4.8)	2.31 dd (6.0, 4.8)	2.31 t (6.0, 4.8)
14	4.14 dd (5.0, 4.5)	4.24 t (4.8)	4.15 t (4.8)	4.09 t (4.8)	4.13 t (4.5)	4.02 t (4.8)	4.20 t (4.8)	4.18 t (4.8)
15a	2.28 dd (15.0, 9.0)	2.24 dd (15.0, 9.0)	2.28 dd (15.0, 9.0)	2.28 dd (15.0, 9.0)	4.25 d (7.0)	4.23 d (6.6)	2.17 dd (13.8, 6.6)	2.20 dd (13.8, 8.4)
15b	2.25 dd (15.0, 6.0)	2.18 dd (15.0, 6.0)	2.15 dd (15.0, 6.0)	2.11 dd (15.0, 6.0)			2.13 dd (13.8, 6.0)	2.17 dd (13.8, 8.4)
16	3.35 m	3.32 m	3.30 m	3.30 m	2.95 brd (7.0)	2.99 brd (6.6)	3.23 m	3.22 t (8.4)
17	3.27 brs	3.29 brs	3.26 brs	3.25 brs	3.28 brs	3.29 brs	3.21 brs	3.19 brs
18a	3.57 d (8.0)	3.21 d (9.0)	3.22 d (9.0)	3.22 d (9.0)	3.48 s	3.53 s	3.15 d (9.0)	3.48 d (8.4)
18b	3.50 d (8.0)	3.15 d (9.0)	3.17 d (9.0)	3.17 d (9.0)	3.48 s	3.53 s	3.10 d (9.0)	3.45 d (8.4)
19a	3.39 d (12.5)	2.98 d (12.6)	2.99 d (12.6)	2.98 d (13.2)	3.40 d (12.0)	3.44 d (13.2)	2.90 d (12.6)	3.38 d (12.0)
19b	3.06 d (12.5)	2.88 d (12.6)	2.89 d (12.6)	2.89 d (13.2)	2.93 d (12.0)	2.98 d (13.2)	2.85 d (12.6)	2.93 d (12.0)
20a	3.30 m	3.30 dq (12.0, 7.2)	3.30 m	3.30 m	3.27 m	3.30 m	3.26 dq (12.6, 7.2)	3.26 dq (13.2, 7.2)
20b	3.25 m	3.15 dq (12.0, 7.2)	3.15 m	3.14 m	2.98 m	3.02 m	3.07 dq (12.6, 7.2)	3.10 dq (13.2, 7.2)
21	1.43 t (7.5)	1.37 t (7.2)	1.36 t (7.2)	1.35 t (7.2)	1.38 t (7.5)	1.42 t (7.2)	1.30 t (7.2)	1.31 t (7.2)
OCH_3-1							3.32 s	3.30 s
OCH_3-6	3.35 s				3.35 s	3.40 s		3.35 s
OCH_3-16	3.40 s	3.32 s	3.36 s	3.34 s	3.36 s	3.44 s	3.28 s	3.28 s
OCH_3-18	3.32 s	3.32 s	3.33 s	3.33 s	3.27 s	3.32 s	3.27 s	3.26 s
1′	5.11 d (5.5)	4.36 d (6.6)	4.95 d (3.0)	5.05 brs	4.30 d (7.0)	5.04 s	4.32 d (7.2)	4.33 d (7.2)
2′	4.16 dd (8.0, 5.5)	3.59 dd (9.0, 6.6)	3.72 dd (9.0, 3.0)	4.01 brd (1.8)	3.53 dd (9.0, 7.0)	4.00 brd (1.8)	3.55 dd (9.0, 7.2)	3.56 dd (9.0, 7.2)
3′	4.02 dd (8.0, 7.0)	3.49 dd (9.0, 3.6)	3.76 dd (9.0, 3.0)	3.79 dd (3.6, 1.8)	3.45 dd (9.0, 3.0)	3.80 dd (3.6, 1.8)	3.45 dd (9.0, 3.6)	3.46 dd (9.0, 3.6)
4′	3.76 m	3.77 m	3.84 m	4.09 m	3.72 m	4.09 m	3.73 m	3.73 m
5′a	3.75 m	3.84 dd (12.6, 2.4)	3.99 dd (12.0, 1.8)	3.68 dd (11.4, 4.2)	3.80 dd (12.5, 3.0)	3.69 dd (11.4, 3.6)	3.80 dd (12.6, 3.0)	3.80 dd (12.6, 3.0)
5′b	3.65 dd (12.5, 6.5)	3.56 dd (12.6, 1.8)	3.57 dd (12.0, 3.0)	3.64 dd (11.4, 4.8)	3.51 brd (12.5)	3.64 dd (11.4, 5.4)	3.50 dd (12.6, 1.2)	3.50 dd (12.6, 1.2,)

[a]Data were measured in CD_3OD at 500 MHz for **1** and **5** and at 600 MHz for **2**–**4** and **6**–**8**, respectively. Proton coupling constants (J) in Hz are given in parentheses. The assignments were based on ^{1}H–^{1}H COSY, HSQC, and HMBC experiments.

Table 2 ^{13}C NMR spectroscopic data (δ) for compounds **1–8**[a].

No.	1	2	3	4	5	6	7	8
1	77.3	72.2	72.1	72.2	72.5	72.1	82.5	82.3
2	22.6	28.7	28.7	28.7	29.5	29.0	22.2	22.2
3	28.8	26.2	26.2	26.2	28.8	28.4	25.8	28.0
4	39.1	38.8	38.8	38.8	39.8	39.3	38.7	39.2
5	44.2	40.7	40.8	40.8	44.0	43.6	40.5	43.7
6	82.7	26.0	25.9	25.9	84.1	83.6	25.9	82.9
7	55.1	47.6	48.2	48.0	49.2	49.9	47.4	55.0
8	74.6	75.2	74.9	75.0	79.4	78.9	75.2	74.7
9	48.0	43.9	45.9	44.6	46.8	46.8	43.9	45.2
10	45.3	44.8	44.7	44.6	45.4	44.7	45.0	45.2
11	52.1	50.6	50.5	50.5	51.6	51.0	51.3	52.1
12	31.0	30.5	29.8	30.2	31.6	30.8	30.4	30.7
13	41.3	41.0	38.9	41.1	41.0	40.9	40.9	41.0
14	76.0	81.5	81.5	80.7	82.3	81.0	81.4	81.6
15	41.8	42.3	42.3	42.4	79.6	79.4	42.3	42.0
16	83.6	84.1	83.8	84.2	93.0	93.1	84.0	83.9
17	66.7	65.4	65.6	65.5	64.7	64.2	64.5	63.8
18	80.0	78.9	79.0	78.9	80.3	79.8	78.7	79.7
19	58.6	57.8	57.8	57.8	59.4	58.9	58.1	59.3
20	50.9	50.1	50.1	50.1	51.0	50.5	50.1	50.1
21	10.3	10.6	10.7	10.7	11.3	10.9	10.6	10.7
OCH_3-1							56.3	56.0
OCH_3-6	58.5				59.0	58.5		58.6
OCH_3-16	56.5	56.5	56.6	56.5	58.0	57.6	56.5	56.5
OCH_3-18	59.5	59.6	59.6	59.6	59.9	59.5	59.6	59.5
1′	97.7	103.1	100.3	109.2	103.9	109.4	103.1	103.2
2′	77.9	72.2	70.7	81.7	72.7	82.0	72.2	72.2
3′	75.8	74.7	71.5	79.1	75.2	79.1	74.7	74.6
4′	84.0	69.8	70.2	87.7	70.4	87.5	69.8	69.7
5′	63.6	67.2	64.8	63.4	67.9	63.4	67.2	67.1

[a]Data were measured in CD_3OD at 125 MHz for **1** and **5** and at 150 MHz for **2–4** and **6–8**, respectively. The assignments were based on $^1H–^1H$ COSY, HSQC, and HMBC experiments.

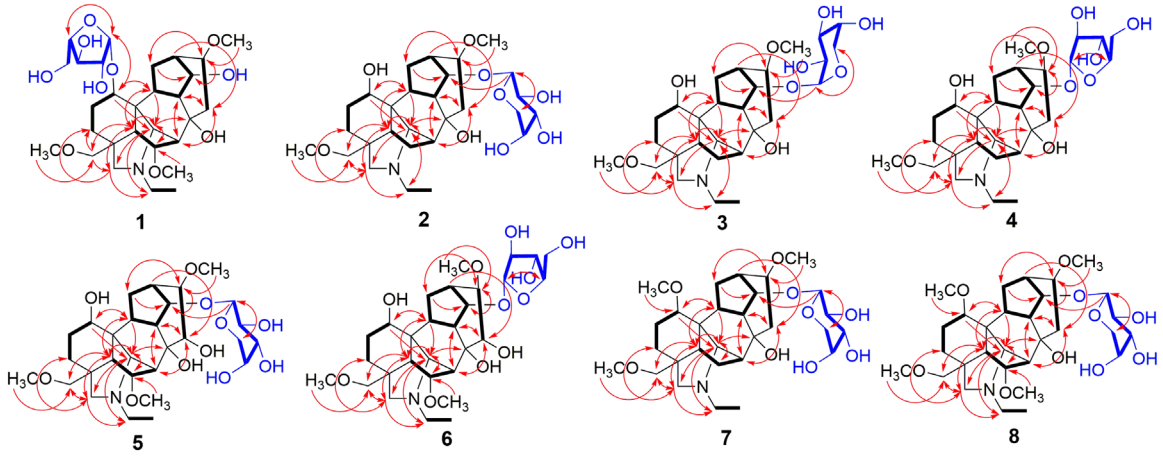

Figure 2 Main $^1H–^1H$ COSY (thick lines) and three-bond HMBC (arrows, from ^1H to ^{13}C) correlations of compounds **1–8**.

was substituted by an oxymethine [δ_H 4.25 (d, J = 7.0 Hz) and δ_C 79.6] in **5**, while the chemical shift of C-16 in **5** was deshielded significantly by $\Delta\delta_C$ +9.4. This revealed that the aglycone in **5** was 15α-hydroxyneoline (fuziline). Additionally, the chemical shifts and coupling patterns of the arabinosyl moiety in **5** were completely different from those of β-arabinofuranosyl in **1**, but were well consistent with those of α-arabinopyranosyl in **2**. Accordingly, compound **5** was elucidated as a fuziline α-arabinopyranoside. The deduction was further verified by 2D NMR data analysis of **5** (Figs. 2 and 3). Especially the $^1H–^1H$ COSY cross-peaks between H-15 and H-16 and the HMBC correlations from H-15 to C-16 and C-8 and from H-16 to C-12, C-14, and C-15, together with their chemical shifts, confirmed the location of the hydroxy group at C-15. The HMBC correlations from H-1′ to

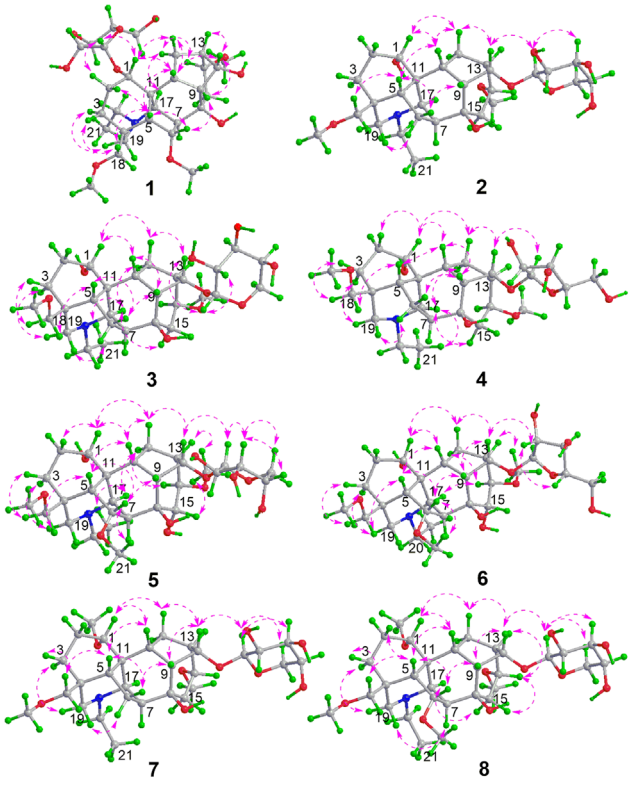

Figure 3 Main NOE correlations (pink dashed double arrows) of compounds **1**–**8**.

C-14, from H_2-5′ to C-1′, and from H-14 to C-1′ located the *α*-arabinopyranosyl at C-14 in **5**. The NOESY correlations supported that the aglycone configuration was identical to fuziline.[50] The configuration was further confirmed by isolation and identification of fuziline and L-arabinose from the acid hydrolysate of **5**. Therefore, the structure of compound **5** was determined as fuziline 14-*O*-*α*-L-arabinopyranoside and named aconicarmichoside I.

Compound **6** was obtained as a colorless gum with $[\alpha]_D^{20}$ –19.8 (*c* 0.12, MeOH). As compared, the NMR spectroscopic data for the aglycone of **6** were well consistent with those of **5**, whereas the data for the pentosyl were almost overlapped with those of **4** (Tables 1 and 2). Thus, **6** was elucidated as the isomer of **5** with replacement of the *α*-L-arabinopyranosyl by an *α*-L-arabinofuranosyl. This was proved by analysis of the 2D NMR spectroscopic data of **6** (Figs. 2 and 3). Therefore, the structure of compound **6** was determined as fuziline 14-*O*-*α*-L-arabinofuranoside and named aconicarmichoside J.

Compound **7**, a colorless gum with $[\alpha]_D^{20}$ –50.9 (*c* 0.43, MeOH), has the molecular formula $C_{29}H_{47}NO_9$ as indicated from (+)-HR-ESI-MS and NMR spectroscopic data. The NMR spectroscopic data of **7** were similar to those of **2**, except for resonances attributable to an additional methoxy group (δ_H 3.32 and δ_C 56.3). In addition, as compared with those of **2**, the H-1 and C-1 and C-2 resonances of **7** were significantly shifted by $\Delta\delta_H$ −0.48 and $\Delta\delta_C$ +10.3 and −6.5, respectively. These differences suggest that **7** is the 1-*O*-methyl ether of **2**, *e.g.,* the aglycone of **7** is 1-*O*-methylisotalatizidine (talatizamine).[51] The suggestion was proved by 2D NMR spectroscopic data of **7** (Figs. 2 and 3). Especially the HMBC correlations from OCH_3-1 to C-1, from OCH_3-16 to C-16, and from OCH_3-18 to C-18 positioned the three methoxy groups in **7**, while the HMBC correlations from H-1′ to C-14 and from H-14 to C-1′ located *α*-L-arabinopyranosyl at C-14. Hence, the structure of compound **7** was determined as talatizamine 14-*O*-*α*-L-arabinopyranoside and named aconicarmichoside K.

Compound **8** was obtained as a colorless gum with $[\alpha]_D^{20}$ –5.5 (*c* 0.11, MeOH). Its spectroscopic data indicated that this compound was another C_{19}-diterpenoid alkaloid *α*-L-arabinopyranoside. Comparison the NMR spectroscopic data between **8** and **7** demonstrated the presence of one more methoxy group (δ_H 3.35 and δ_C 58.6) in **8** and replacement of one methylene (CH_2-6) in **7** by an oxymethine (δ_H 4.29 and δ_C 82.9) in **8**. In addition, the H-5 resonance was changed from the broad singlet at δ_H 2.04 in **7** to a doublet at δ_H 2.35 (J = 6.6 Hz), and the H-18a, H-18b, and H-19a and C-7 resonances were significantly deshielded by $\Delta\delta_H$ +0.33, +0.35, and +0.48 and $\Delta\delta_C$ +7.6, respectively. This indicated that **8** was the 6-methoxy analogue of **7**, which was supported by comparison of the NMR spectroscopic data of **8** with the reported data for the aglycone (6-methoxytalatizamine, chasmanine)[51] and further confirmed by 2D NMR spectroscopic data analysis (Figs. 2 and 3). Therefore, the structure of compound **8** was determined as chasmanine 14-*O*-*α*-L-arabinopyranoside and named aconicarmichoside L.

Although the aglycones and sugar have positive specific rotations except for talatizamine {$[\alpha]_D^{20}$ –4.4 (*c* 1.0, $CHCl_3$)}[51], the *β*-L-arabinosides **1** and **3** have the positive data, whereas the *α*-L-arabinosides **2** and **4**–**8** have the larger negative data. This is consistent with that previously observed for neoline L-arabinosides[48], suggesting that the C-1′ configuration of L-arabinosyl plays a decisive role in the specific rotations. Accordingly, the specific rotation data are valuable to preliminarily assign the configurations of the C_{19}-diterpenoid alkaloid arabinosides. This was supported by acid hydrolysis of the neoline L-arabinoside isomers[48] as well as of **2**, **3**, and **5**. Because the absolute configuration of the co-occurring aglycones, including neoline[52–54], isotalatizidine[55], fuziline[50], talatizamine,[5,51] and chasmanine[51–54], were previously determined by chemical transformation and/or X-ray crystallography, the structures as shown in Fig. 1 represent the absolute configurations of **1**–**8**. Additionally, based on the splitting pattern of H-1 in the ^{1}H NMR spectra (Table 1), the ring A in **1**–**8** has a boat conformation in CD_3OD[52,53], which is consistent with that of the aglycones in crystals[50,54,55].

Because the ring A conformation in solution may be affected by the presence of acid in the samples[43,52,53,56] and because trifluoroacetic acid (TFA) was used in the isolation procedure, compounds **1**–**8** were suspected to be obtained as trifluoroacetates[57–59]. Although the ^{13}C NMR spectra of **1**–**8** did not displayed the corresponding resonances of TFA, the presence of TFA in the samples were confirmed by the ^{19}F NMR spectra. Furthermore, using benzene (C_6H_6) and hexafluorobenzene (C_6F_6) as internal standards, ratios of the alkaloid and TFA in these samples were estimated to be 1:0.8 to 1:3.1 (Supplementary Information Figs. S107–S122). To preliminarily explore the influence of TFA on the ring conformations, the NMR spectra of **2** and **7** in pyridine-d_5 were acquired. As shown in Figs. 4 and 5, comparing with those of the same samples in CD_3OD, intensity and resolution of some resonances especially for the ring A and *N*-Et moieties in **7** were significantly decreased or disappeared in pyridine-d_5. However, this phenomenon was not observed for **2**. The results demonstrated that (a) the different conformations of the ring A and *N*-Et moieties in **7** were relatively slowly transformed during the time scale of the NMR detection under the basic condition of pyridine-d_5, (b) TFA

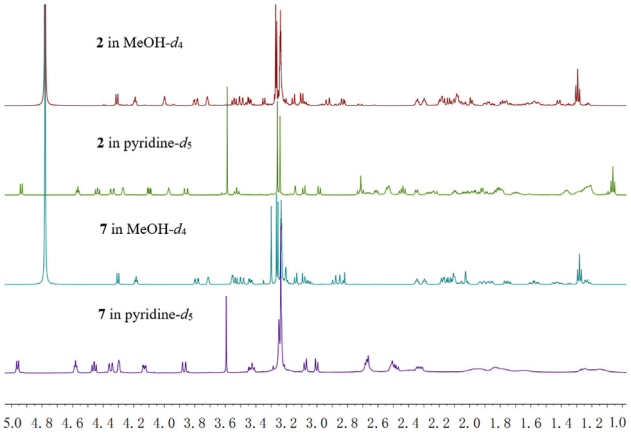

Figure 4 The overlaid ^{1}H NMR spectra of **2** and **7** (600 MHz) in CD_3OD and pyridine-d_5. The same samples **2** (3.0 mg) and **7** (2.0 mg) were repeatedly used after evaporation under reduced pressure. The same volume (0.6 mL) of the solvents was applied.

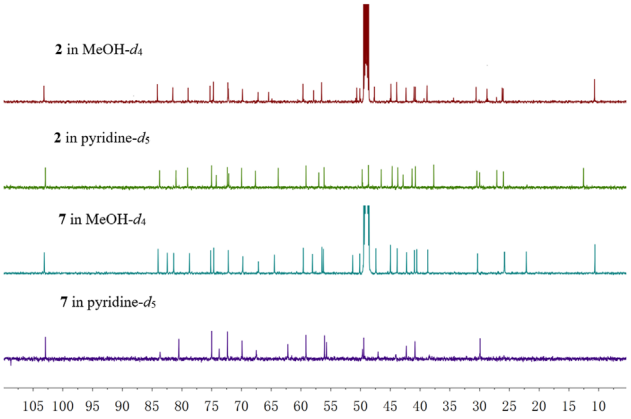

Figure 5 The overlaid ^{13}C NMR spectra of **2** and **7** (150 MHz) in CD_3OD and pyridine-d_5. The same samples **2** (3.0 mg) and **7** (2.0 mg) were repeatedly used after evaporation under reduced pressure. The same volume (0.6 mL) of the solvents was applied.

containing in the sample of **7** should play an important role to stabilize the conformation in CD_3OD, (c) an intramolecular hydrogen bonding between 1-OH and nitrogen atom would be the key fact to stabilize the conformation of **2**, since **2** and **7** differ only in replacement of 1-OH in **2** by 1-OCH_3 in **7** and since the conformation of **2** was unchanged in the two solvents. This, together with our previous observations[43,46,47], indicates that acids and bases may cause conformational and/or structural changes of the diterpenoid alkaloids. However, the changes are highly dependent upon the chemical structures of the diterpenoid alkaloids. Because TFA was undoubtedly introduced during the experimental procedure, the structure assignments of the diterpenoid alkaloids **1**–**8** were unambiguous though the samples contained the different amounts of TFA and possible formation of trifluoroacetates and/or equilibration of dissociation in solution could not be excluded. Notably, having alkali properties, in hydrophilic bio-systems the diterpenoid alkaloids would interact with the endogenous acidic and basic biomolecules or microenvironments to increase solubility, bioavailability, and transportations as well as to play biological functions. This deserves further investigations on a case by case basis.

Based on clinic application of "Fu Zi", the analgesic effects of compounds **1**, **2**, and **4**–**8** were evaluated using acetic acid-induced writhing assay[60] except for **3** due to limitation of the small sample amount. As shown in Table 3 and Fig. 6, at doses of 1.0, 0.3, and 0.1 mg/kg (i.p.), as compared with the vehicle group, **1**, **2**, and **4**–**6** exhibited significant reduction of writhing of mice in a dose-dependent manner. However, compounds **7** and **8** showed weak activity with $<20\%$ inhibition of writhes at the high dose of 1.0 mg/kg (i.p.). This result indicated that the structural change of the L-arabinosyl moieties in **1**, **2**, and **4**–**6** and the absence of the methoxy group at C-6 in **2** and **4** had little influence on the analgesic activity. Whereas, methylation of the hydroxyl group at C-1 (**7** and **8**) significantly decreased the activity.

3. Conclusions

Eight new aconitine-type C_{19}-diterpenoid alkaloid L-arabinosides (**1**–**8**) were isolated and characterized from the lateral roots of *A. carmichaelii* (Fu Zi). These compounds, together with four neoline 14-*O*-arabinosides from the same extract[48], are the only glycosidic diterpenoid alkaloids, though around a thousand C_{20}-, C_{19}-, and C_{18}-diterpenoid alkaloids have been isolated from nature[49]. This finding not only adds diversity of the bioactive diterpenoid alkaloids, but also provides a solid evidence for the occurrence of glycosidation of the diterpenoid alkaloids in plant. The analgesic effects of **1**, **2**, and **4**–**6** supports clinic application of the traditional herbal medicine, and provides candidates for new drug development. In addition, the structure–activity relationship observed in this study directs a rational path for structural modification of the C_{19}-diterpenoid alkaloids to improve their biological and pharmaceutical properties.

4. Experimental

4.1. General experimental procedures

Optical rotations were measured on P-2000 polarimeter (JASCO, Tokyo, Japan). IR spectra were recorded on a Nicolet 5700 FT-IR microscope instrument (FT-IR microscope transmission) (Thermo Electron Corporation, Madison, WI, USA). NMR spectra were obtained at 500 MHz or 600 MHz for ^{1}H NMR, 125 MHz or 150 MHz for ^{13}C NMR, and 470 MHz for ^{19}F NMR respectively, on Inova 500 or SYS 600 (Varian Associates Inc., Palo Alto, CA, USA), or Bruker 600 NMR, Bruker 500 NMR (Bruker Corp. Karlsruhe, Germany) spectrometer in MeOH-d_4, D_2O, or pyridine-d_5 with TMS or solvent peaks as references. ESI-MS and HR-ESI-MS data were obtained on Agilent 1100 Series LC-MSD-Trap-SL and Agilent 6520 Accurate-Mass Q-TOFL CMS spectrometers (Agilent Technologies, Ltd., Santa Clara, CA, USA), respectively. Column chromatography (CC) was performed with macroporous adsorbent resin (HPD-100, Cangzhou Bon Absorber Technology Co., Ltd., Cangzhou, China), MCI gel (CHP 20P, 75–150 μm, Mitsubishi Chemical Inc., Tokyo, Japan), silica gel (200–300 mesh, Qingdao Marine Chemical Inc., Qingdao, China), Sephadex LH-20 (Pharmacia Biotech AB, Uppsala, Sweden), or CHP 20P (Mitsubishi Chemical Inc., Tokyo, Japan). HPLC separation was performed on a system consisting of an Agilent ChemStation for LC system, an Agilent 1200 pump, and an Agilent 1100 single-wavelength absorbance detector (Agilent Technologies, Ltd.) or a Smartline RI detector (Knauer, Berlin, Germany) detector, using

Table 3 Experimental data for the analgesic effect of compounds **1**, **2**, and **4–8**.

Group	Reagent	Dose (mg/kg)	Number of writhing	Percent inhibition (%)
Vehicle group	Normal saline	–	38.9 ± 5.58	–
Positive group	Morphine	0.3	18.3 ± 1.60***	65.47
Test group	**1**	0.1	20.1 ± 3.28**	43.15
		0.3	12.8 ± 4.24**	63.63
		1.0	7.80 ± 2.58***	78.34
	2	0.1	31.4 ± 4.75	19.23
		0.3	14.3 ± 3.54**	63.34
		1.0	12.3 ± 2.07***	68.39
	4	0.1	15.3 ± 5.54**	60.56
		0.3	15.7 ± 3.06**	59.61
		1.0	13.4 ± 2.76***	65.59
	5	0.1	25.67 ± 4.32	27.49
		0.3	12.8 ± 2.98***	63.84
		1.0	11.7 ± 3.09***	67.04
	6	0.1	11.2 ± 4.35***	68.36
		0.3	13.1 ± 2.68**	62.87
		1.0	9.1 ± 2.53***	74.22
	7	1.0	29.0 ± 2.07	20.01
	8	1.0	29.4 ± 3.85	13.82

–Not applicable. Data are expressed as mean ± SEM, $n = 10$.
**$P < 0.01$.
***$P < 0.001$ compared to model group.

an Ultimate XB-Phenyl column (250 mm × 10 mm i.d.) packed with phenyl-silica gel (5 mm) (Welch, shanghai, China). TLC was conducted on precoated silica gel GF_{254} plates. Spots were visualized under UV light (254 or 365 nm) or by spraying with 7% H_2SO_4 in 95% EtOH followed by heating or with a Dragendorff's reagent. Unless otherwise noted, all chemicals were obtained from commercially available sources and were used without further purification.

4.2. Plant material

The lateral root of *A. carmichaelii* Debx was collected in June 2009 from the culture field in Jiangyou, Sichuan Province, China. Plant identity was verified by Dr. Yan Ren (Chengdu University of Traditional Chinese Medicine, Sichuan 610075, China). A voucher specimen (No. ID-S-2383) was deposited at the herbarium of Natural Medicinal Chemistry, Institute of Materia Medica.

4.3. Extraction and isolation

The air-dried lateral roots of *A. carmichaelii* (50 kg) were powdered and extracted with H_2O (3 × 150 L × 6 h) at 40 °C. The H_2O extract was concentrated to 120 L under reduced pressure, subjected to chromatography over a macroporous adsorbent resin (HPD-110, 19 kg) column (200 cm × 20 cm), and eluted successively with H_2O (50 L), 30% EtOH (120 L), 50% EtOH (120 L), and 95% EtOH (100 L) to afford the corresponding fractions A–D. After removal of the solvent, fraction C (3.5 kg) was chromatographed over MCI gel (CHP 20 P) with successive elution using H_2O (10 L), 30% EtOH (30 L), 50% EtOH (20 L), and 95% EtOH (10 L) to give fraction C1–C4. Fraction C2 (600 g) was chromatographed over MCI gel (CHP 20 P), with successive elution using H_2O (10 L), 30% EtOH (30 L), 50% EtOH (20 L), and 95% EtOH (10 L), to yield corresponding subfractions C2-1–C2-4. Fraction C2-1 (200 g) was dissolved in H_2O (500 mL), basified to pH 10 with concentrated ammonium hydroxide (25 mL), then extracted with EtOAc (500 mL × 4). The aqueous layer was acidified to pH 4 with 6 mol/L HCl (66 mL), and partitioned with *n*-butanol (500 mL × 3). Evaporation of the aqueous phase under reduced pressure yielded C2-1-C (32 g). Fraction C2-1-C was subjected to CC over silica gel, eluting with a gradient of $CHCl_3$-CH_3OH (50:1–0:1) to afford C2-1-C-1–C2-1-C-6. Fraction C2-1-C-4 (4 g) was separated by CC over Sephadex LH-20 (MeOH) to yield C2-1-C-4-1–C2-1-C-4-6, of which C2-1-C-4-4 (2 g) was further fractionated by CC over Sephadex LH-20 (50% MeOH in H_2O) to give C2-1-C-4-4-1–C2-1-C-4-4-4. Separation of C2-1-C-4-4-1 (340 mg) by reverse phase C-18 silica gel (10–90% MeOH in H_2O) afforded C2-1-C-4-4-1-1–C2-1-C-4-4-1-5, of which C2-1-C-4-4-1-1 (66 mg) was separated by CC over silica gel, eluting with a gradient of EtOAc–MeOH–H_2O (8:3:1–8:4:1), to obtain C2-1-C-4-4-1-1-1 and C2-1-C-4-4-1-1-2. Purification of C2-1-C-4-4-1-1-1 (30.6 mg) by reversed phase HPLC (Ultimate XB-phenyl semi-preparative column, 28% MeOH in H_2O, containing 0.1% TFA, 2 mL/min) obtained **7** (3 mg, t_R = 45 min). Fraction C2-1-C-4-4-1-3 (20 mg) was isolated by HPLC using the same column (40% MeOH in H_2O containing 0.2% TFA, 2 mL/min) to obtain **8** (3.4 mg, t_R = 27 min). Fraction C2-1-C-5 (13.0 g) was separated by CC over Sephadex LH-20 (H_2O) to give C2-1-C-5-1–C2-1-C-5-6, of which C2-1-C-5-4 (4 g) was further fractionated by CC over Sephadex LH-20 (H_2O) to afford C2-1-C-5-4-1–C2-1-C-5-4-7. Fraction C2-1-C-5-4-6 (1.1 g) was separated by CC over reverse phase C-18 silica gel (0–50% MeOH in H_2O) to give C2-1-C-5-4-6-1–C2-1-C-5-4-6-5, of which C2-1-C-5-4-6-3 (53.7 mg) was purified by reversed phase HPLC (30% MeOH in H_2O, containing 0.1% TFA, 2 mL/min) to yield **2** (10.4 mg, t_R = 45 min).

Fraction C2-2 (200 g) was separated by CC over Sephadex LH-20 ($CHCl_3$-MeOH, 1:1) yielded C2-2-1–C2-2-8. Fraction C2-2-4 (9.5 g) was chromatographed over silica gel (150 g) eluting with a

gradient of petroleum ether-Me_2CO-diethylamine (5:2:1–2:2:1) to give C2-2-4-1–C2-2-4-7. Fraction C2-2-4-6 (2.65 g) was separated by CC over silica gel, eluting with a gradient of $CHCl_3$ (saturated with ammonia water)–MeOH (20:1–5:1), to give C2-2-4-6-1–C2-2-4-6-11, of which C2-2-4-6-6 (1.5 g) was further fractionated by CC over reversed phase C-18 silica gel (30%–50% MeOH in H_2O) to give C2-2-4-6-6-1–C2-2-4-6-6-3. Fraction C2-2-4-6-6-1 (1.2 g) was subjected to preparative TLC [$CHCl_3$ (saturated with ammonia water)–MeOH, 5:1] to yield C2-2-4-6-6-1-1 and C2-2-4-6-6-1-2. Further separation of C2-2-4-6-6-1-1 (0.9 g) by reversed phase HPLC (15% MeCN in H_2O containing 0.1% TFA, 2 mL/min) yielded C2-2-4-6-6-1-1-1–C2-2-4-6-6-1-1-5, of which C2-2-4-6-6-1-1-2 (250 mg) was separated by HPLC (10% MeCN in H_2O containing 0.1% TFA, 2 mL/min) to yielded C2-2-4-6-6-1-1-2-1–C2-2-4-6-6-1-1-2-5. Fraction C2-2-4-6-6-1-1-2-4 (38 mg) was isolated by HPLC (25% MeOH in H_2O containing 0.1% TFA, 2 mL/min) yield **4** (6.5 mg, t_R = 70 min). Fraction C2-2-4-6-6-1-1-2-5 (20 mg) was separated by HPLC (30% MeOH in H_2O containing 0.1% TFA, 2 mL/min) to yield **3** (1.8 mg, t_R = 48 min). Fraction C2-2-4-6-7 (110 mg) was separated by preparative TLC [$CHCl_3$ (saturated with ammonia water)–MeOH (5:1)] to afford C2-2-4-6-7-1–C2-2-4-6-7-3, of which C2-2-4-6-7-1 (20 mg) was isolated by HPLC (19% acetonitrile in H_2O containing 0.1% TFA, 2 mL/min) to yield **6** (1.5 mg, t_R = 19 min). Fraction C2-2-4-6-8 (110 mg) was separated by HPLC (40% MeOH in H_2O containing 0.1% TFA) to yield C2-2-4-6-8-1–C2-2-4-6-8-11, of which C2-2-4-6-8-3 (76 mg) was fractionated by HPLC (40% MeOH in H_2O containing 0.1% TFA) to afford C2-2-4-6-8-3-1–C2-2-4-6-8-3-4. Compound **1** (3 mg, t_R = 35 min) was isolated from C2-2-4-6-8-3-3 (7 mg) by HPLC (40% MeOH in H_2O, containing 0.1% TFA, 2 mL/min) and **5** (3 mg, t_R = 46 min) from C2-2-4-6-8-4 (65 mg) by HPLC (37% MeOH in H_2O, containing 0.1% TFA, 2 mL/min).

4.3.1. *Aconicarmichoside E (**1**)*

Colorless gum; $[\alpha]_D^{20}$ +25.5 (*c* 0.20, MeOH); IR ν_{max} 3365, 3055, 2925, 2854, 1679, 1631, 1601, 1463, 1421, 1381, 1315, 1243, 1204, 1132, 1040, 1009, 942, 837, 802, 778, 723 cm^{-1}; ^1H NMR (CD_3OD, 500 MHz) spectroscopic data, see Table 1; ^{13}C NMR (CD_3OD, 125 MHz) spectroscopic data, see Table 2; (+)-ESI-MS *m/z* 592 $[M + Na]^+$, 570 $[M + H]^+$; (+)-HR-ESI-MS *m/z* 570.3272 $[M + H]^+$ (Calcd. for $C_{29}H_{48}NO_{10}$, 570.3273).

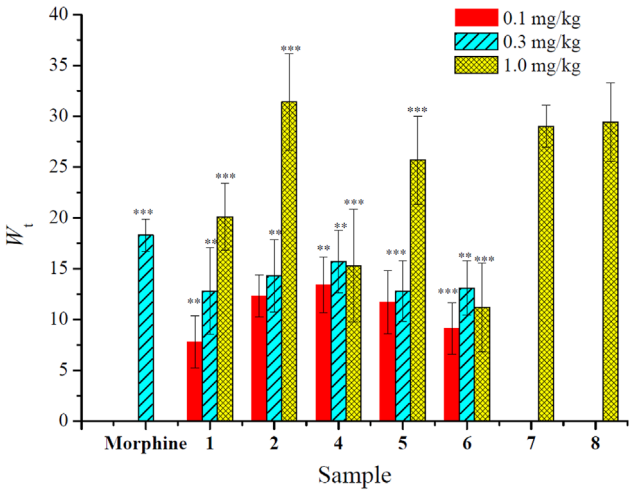

Figure 6 Analgesic effects of compounds **1**, **2**, and **4–8**, and morphine against acetic acid-induced writhing of mice.

4.3.2. *Aconicarmichoside F (**2**)*

Colorless gum; $[\alpha]_D^{20}$ –24.8 (*c* 0.63, MeOH); IR ν_{max} 3408, 1655, 1403, 1194, 1143, 1011, 802, 724 cm^{-1}; ^1H NMR (CD_3OD, 600 MHz) spectroscopic data, see Table 1; ^{13}C NMR (CD_3OD, 150 MHz) spectroscopic data, see Table 2; (+)-ESI-MS *m/z* 540 $[M + H]^+$; (+)-HR-ESI-MS *m/z* 540.3182 $[M + H]^+$ (Calcd. for $C_{28}H_{46}NO_9$, 540.3167).

4.3.3. *Aconicarmichoside G (**3**)*

Colorless gum; $[\alpha]_D^{20}$ +28.3 (*c* 0.14, MeOH); IR ν_{max} 3357, 2923, 2852, 1678, 1468, 1426, 1281, 1205, 1137, 1082, 1011, 841, 801, 723, 634 cm^{-1}; ^1H NMR (CD_3OD, 600 MHz) spectroscopic data, see Table 1; ^{13}C NMR (CD_3OD, 150 MHz) spectroscopic data, see Table 2; (+)-ESI-MS *m/z* 562 $[M + Na]^+$, 540 $[M + H]^+$; (+)-HR-ESI-MS *m/z* 540.3186 $[M + H]^+$ (Calcd. for $C_{28}H_{46}NO_9$, 540.3167).

4.3.4. *Aconicarmichoside H (**4**)*

Colorless gum; $[\alpha]_D^{20}$ –43.7 (*c* 0.40, MeOH); IR ν_{max} 3371, 2946, 1679, 1439, 1204, 1137, 842, 802, 724 cm^{-1}; ^1H NMR (CD_3OD, 600 MHz) spectroscopic data, see Table 1; ^{13}C NMR (CD_3OD, 150 MHz) spectroscopic data, see Table 2; (+)-ESI-MS *m/z* 562 $[M + Na]^+$, 540 $[M + H]^+$; (+)-HR-ESI-MS *m/z* 540.3181 $[M + H]^+$ (Calcd. for $C_{28}H_{46}NO_9$, 540.3167).

4.3.5. *Aconicarmichoside I (**5**)*

Colorless gum; $[\alpha]_D^{20}$ –7.7 (*c* 0.15, MeOH); IR ν_{max} 3334, 2944, 1678, 1436, 1293, 1202, 1136, 1010, 954, 840, 801, 724 cm^{-1}; ^1H NMR (CD_3OD, 500 MHz) spectroscopic data, see Table 1; ^{13}C NMR (CD_3OD, 125 MHz) spectroscopic data, see Table 2; (+)-ESI-MS *m/z* 586 $[M + H]^+$; (+)-HR-ESI-MS *m/z* 586.3239 $[M + H]^+$ (Calcd. for $C_{29}H_{48}NO_{11}$, 586.3222).

4.3.6. *Aconicarmichoside J (**6**)*

Colorless gum; $[\alpha]_D^{20}$ –19.8 (*c* 0.12, MeOH); IR ν_{max} 3358, 2924, 2853, 1678, 1468, 1427, 1311, 1204, 1137, 840, 802, 723 cm^{-1}; ^1H NMR (CD_3OD, 600 MHz) spectroscopic data, see Table 1; ^{13}C NMR (CD_3OD, 150 MHz) spectroscopic data, see Table 2; (+)-ESI-MS *m/z* 586 $[M + H]^+$; (+)-HR-ESI-MS *m/z* 586.3228 $[M + H]^+$ (Calcd. for $C_{29}H_{48}NO_{11}$, 586.3222).

4.3.7. *Aconicarmichoside K (**7**)*

Colorless gum; $[\alpha]_D^{20}$ –50.9 (*c* 0.43, MeOH); IR ν_{max} 3363, 3074, 2926, 1686, 1446, 1381, 1257, 1203, 1136, 1087, 1012, 950, 925, 880, 837, 801, 721 cm^{-1}; ^1H NMR (CD_3OD, 600 MHz) spectroscopic data, see Table 1; ^{13}C NMR (CD_3OD, 150 MHz) spectroscopic data, see Table 2; (+)-ESI-MS *m/z* 554 $[M + H]^+$; (+)-HR-ESI-MS *m/z* 554.3335 $[M + H]^+$ (Calcd. for $C_{29}H_{48}NO_9$, 554.3324).

4.3.8. *Aconicarmichoside L (**8**)*

Colorless gum; $[\alpha]_D^{20}$ –5.5 (*c* 0.11, MeOH); IR ν_{max} 3366, 2942, 1684, 1444, 1378, 1202, 1139, 1078, 1010, 953, 844, 801, 724 cm^{-1}; ^1H NMR (CD_3OD, 600 MHz) spectroscopic data, see Table 1; ^{13}C NMR (CD_3OD, 150 MHz) spectroscopic data, see Table 2; (+)-ESI-MS *m/z* 584 $[M + H]^+$; (+)-HR-ESI-MS *m/z* 584.3437 $[M + H]^+$ (Calcd. for $C_{30}H_{50}NO_{10}$, 584.3429).

4.4. Acid hydrolysis of **2**, **3**, and **5**

Compounds **2**, **3**, and **5** (2–5 mg, each) were separately dissolved in acetonitrile (0.1 mL), and hydrolyzed in 2 mol/L HCl (2.0 mL) at 95 °C for 3 h. After evaporation under reduced pressure, the residue was chromatographed by CC over Sephadex LH-20 (MeOH) to yield aglycone (0.8–2.3 mg) and sugar (0.5–1.6 mg). By comparison of the ^{1}H NMR spectroscopic data (Supplementary Information Figs. S25–S29, S42, S43, and S68–S70) and specific rotation with those of authentic diterpenoid alkaloid samples previously isolated in this study and commercially available sugar samples, the aglycones were identified as isotalatizidine {$[\alpha]_D^{20}$ +23.4 (*c* 0.09, MeOH) and +21.5 (*c*, 0.05, MeOH)} from **2** and **3** and fuziline {$[\alpha]_D^{20}$ +8.2 (*c* 0.04, MeOH)} from **5**, respectively, while the sugar from the three compounds was identified as L-arabinose {$[\alpha]_D^{20}$ +96.6 to +106.3 (*c* 0.05–0.10, H_2O).

4.5. Acetic acid-induced writhing test

An acetic acid-induced writhing method was adopted for the evaluation of analgesic activity. Briefly, ICR female mice were randomly divided into five groups (10 mice per group), and pre-treated intraperitoneally with normal saline (the vehicle group), morphine (0.3 mg/kg, the positive control group), and each compound (1.0 mg/kg, 0.3 mg/kg, and 0.1 mg/kg, the three test groups), respectively. 30 min later, mice were treated by intraperitoneal injection of 1.0% *v/v* acetic acid solution (0.1 mL/kg). The number of writhing was recorded for 15 min. The analgesic effects of the test compounds and positive control were respectively expressed by decreasing the number of writhes compared to normal saline. Percent inhibition was calculated using formula as below:

$$\text{Percent inhibition } (\%) = \left[(W_m - W_t)/W_m\right] \times 100$$

where W_m is the number of writhing of the vehicle group, and W_t is the number of writhing of test group or positive group. The results (Fig. 6 and Table 3) showed that compounds **1**, **2**, and **4–6** significantly reduced the writhes induced by acetic acid in a dose-dependent manner.

Acknowledgments

Financial support from the National Natural Sciences Foundation of China (81630094, 21732008, 81373388, and 81573445) and CAMS Innovation Fund for Medical Science (2017-I2M-3–010, 2016-I2M-1–004, 2016-I2M-1–010, and 2017-I2M-3–011) is acknowledged.

Appendix A. Supporting information

Supplementary data associated with this article can be found in the online version at doi:10.1016/j.apsb.2018.03.009.

References

1. Jiangsu New Medical College. *Dictionary of traditional Chinese medicine*. Shanghai: Shanghai Science and Technology Publishing House; 1995 . p. 228–232, and 1191-4.
2. Chen Y, Chu YL, Chu JH. Alkaloids of the Chinese drugs, *Aconitum* spp.—IX. Alkaloids from Chuan-Wu and Fu-Tzu, *Aconitum carmichaeli* Debx. *Acta Pharm Sin* 1965;**12**:435–9.
3. Iwasa J, Naruto S. Alkaloids from *Aconitum carmichaeli* DEBX. *J Pharm Soc Jpn* 1966;**86**:585–90.
4. Shim SH, Lee SY, Kim JS, Son KH, Kang SS. Norditerpenoid alkaloids and other components from the processed tubers of *Aconitum carmichaeli*. *Arch Pharm Res* 2005;**28**:1239–43.
5. Konno C, Shirasaka M, Hikino H. Structure of senbusine A, B and C, diterpenie alkaloids of *Aconitum carmichaeli* roots from China. *J Nat Prod* 1982;**45**:128–33.
6. Zhang WD, Han GY, Liang HQ. Studies on the alkaloid constituents of Jiangyou Fu-zi *Aconitum carmichaeli* from Sichuan. *Acta Pharm Sin* 1992;**27**:670–3.
7. Wang XK, Zhao TF, Lai S. A new N-formyl C_{19}-diterpenoid alkaloid, aldohypaconitine, from cultivated *Aconitum carmichaeli*, Debx. *Chin Chem Lett* 1994;**5**:671–2.
8. Xiong J, Gu K, Tan NH. Diterpenoid alkaloids from the processed roots of *Aconitum carmichaeli*. *Nat Prod Res Dev* 2008;**20**:440–3, 465.
9. Liu XX, Jian XX, Cai XF, Chao RB, Chen QH, Chen DL, et al. Cardioactive C_{19}-diterpenoid alkaloids from the lateral roots of *Aconitum carmichaeli* "Fu Zi". *Chem Pharm Bull* 2012;**60**:144–9.
10. Gao F, Li YY, Wang D, Huang X, Liu Q. Diterpenoid alkaloids from the Chinese traditional herbal "Fuzi" and their cytotoxic activity. *Molecules* 2012;**17**:5187–94.
11. Zhang J, Sun GB, Lei QF, Li GZ, Wang JC, Si JY. Chemical constituents of lateral roots of *Aconitum carmichaelii* Debx. *Acta Pharm Sin* 2014;**49**:1150–4.
12. Zhou G, Tang L, Zhou X, Wang T, Kou Z, Wang Z. A review on phytochemistry and pharmacological activities of the processed lateral root of *Aconitum carmichaelii* Debeaux. *J Ethnopharmacol* 2015;**160**:173–93.
13. Chang YT, Wu JY, Liu TP. On the toxicity of Fu-Tze (*Aconitum chinense*). *Acta Pharm Sin* 1966;**13**:350–5.
14. Bisset NG. Arrow poisons in China. Part II. *Aconitum*-botany, chemistry, and pharmacology. *J Ethnopharmacol* 1981;**4**:247–336.
15. Zhou YP. Pharmacological effects and toxicities of Fuzi and its main chemical constituents. *Acta Pharm Sin* 1983;**18**:394–400.
16. Chan TY. Aconite poisoning. *Clin Toxicol* 2009;**47**:279–85.
17. Jiang ZB, Song WX, Shi JG. Two 1-(6′-O-acyl-β-D-glucopyranosyl) pyridinium-3-carboxylates from the flower buds of *Lonicera japonica*. *Chin Chem Lett* 2015;**26**:69–72.
18. Yu Y, Jiang Z, Song W, Yang Y, Li Y, Jiang J, et al. Glucosylated caffeoylquinic acid derivatives from the flower buds of *Lonicera japonica*. *Acta Pharm Sin B* 2015;**5**:210–4.
19. Song WX, Guo QL, Yang YC, Shi JG. Two homosecoiridoids from the flower buds of *Lonicera japonica*. *Chin Chem Lett* 2015;**26**:517–21.
20. Jiang Y, Liu Y, Guo Q, Jiang Z, Xu C, Zhu C, et al. Acetylenes and fatty acids from *Codonopsis pilosula*. *Acta Pharm Sin B* 2015;**5**:215–22.
21. Jiang YP, Liu YF, Guo QL, Jiang ZB, Xu CB, Zhu CG, et al. C_{14}-polyacetylene glucosides from *Codonopsis pilosula*. *J Asian Nat Prod Res* 2015;**17**:601–14.
22. Jiang YP, Liu YF, Guo QL, Shi JG. C_{14}-polyacetylenol glycosides from the roots of *Codonopsis pilosula*. *J Asian Nat Prod Res* 2015;**17**:1166–79.
23. Jiang YP, Guo QL, Liu YF, Shi JG. Codonopiloneolignanin A, a polycyclic neolignan with a new carbon skeleton from the roots of *Codonopsis pilosula*. *Chin Chem Lett* 2016;**27**:55–8.
24. Jiang Y, Liu Y, Guo Q, Xu C, Zhu C, Shi J. Sesquiterpene glycosides from the roots of *Codonopsis pilosula*. *Acta Pharm Sin B* 2016;**6**:46–54.
25. Guo Q, Wang Y, Lin S, Zhu C, Chen M, Jiang Z, et al. 4-Hydroxybenzyl-substituted amino acid derivatives from *Gastrodia elata*. *Acta Pharm Sin B* 2015;**5**:350–7.
26. Guo QL, Wang YN, Zhu CG, Chen MH, Jiang ZB, Chen NH, et al. 4-Hydroxybenzyl-substituted glutathione derivatives from *Gastrodia elata*. *J Asian Nat Prod Res* 2015;**17**:439–54.

27. He J, Luo Z, Huang L, He J, Chen Y, Rong X, et al. Ambient mass spectrometry imaging metabolomics method provides novel insights into the action mechanism of drug candidates. *Anal Chem* 2015;**87**:5372–9.
28. Guo QL, Lin S, Wang YN, Zhu CG, Xu CB, Shi JG. Gastrolatathioneine, an unusual ergothioneine derivative from an aqueous extract of "tian ma": a natural product co-produced by plant and symbiotic fungus. *Chin Chem Lett* 2016;**27**:1577–81.
29. Liu Z, Wang W, Feng N, Wang L, Shi J, Wang X. Parishin C's prevention A$\beta_{1\text{-}42}$-induced inhibition of long-term potentiation is related to NMDA receptors. *Acta Pharm Sin B* 2016;**6**:189–97.
30. Zhou X, Guo QL, Zhu CG, Xu CB, Wang YN, Shi JG. Gastradefurphenol, a minor 9,9'-neolignan with a new carbon skeleton substituted by two *p*-hydroxybenzyls from an aqueous extract of "tian ma". *Chin Chem Lett* 2017;**28**:1185–9.
31. Liu YF, Chen MH, Wang XL, Guo QL, Zhu CG, Lin S, et al. Antiviral enantiomers of a bisindole alkaloid with a new carbon skeleton from the roots of *Isatis indigotica*. *Chin Chem Lett* 2015;**26**:931–6.
32. Liu YF, Chen MH, Guo QL, Lin S, Xu CB, Jiang YP, et al. Antiviral glycosidic bisindole alkaloids from the roots of *Isatis indigotica*. *J Asian Nat Prod Res* 2015;**17**:689–704.
33. Liu YF, Chen MH, Lin S, Li YH, Zhang D, Jiang JD, et al. Indole alkaloid glucosides from the roots of *Isatis indigotica*. *J Asian Nat Prod Res* 2016;**18**:1–12.
34. Liu Y, Wang X, Chen M, Lin S, Li L, Shi J. Three pairs of alkaloid enantiomers from the root of *Isatis indigotica*. *Acta Pharm Sin B* 2016;**6**:141–7.
35. Chen MH, Lin S, Wang YN, Zhu CG, Li YH, Jiang JD, et al. Antiviral stereoisomers of 3,5-bis(2-hydroxybut-3-en-1-yl)-1,2,4-thiadiazole from the roots of *Isatis indigotica*. *Chin Chem Lett* 2016;**27**:643–8.
36. Li DW, Guo QL, Meng XH, Zhu CG, Xu CB, Shi JG. Two pairs of unusual scalemic enantiomers from *Isatis indigotica* leaves. *Chin Chem Lett* 2016;**27**:1745–50.
37. Liu Y, Chen M, Guo Q, Li Y, Jiang J, Shi J. Aromatic compounds from an aqueous extract of "ban lan gen" and their antiviral activities. *Acta Pharm Sin B* 2017;**7**:179–84.
38. Meng L, Guo Q, Liu Y, Chen M, Li Y, Jiang J, et al. Indole alkaloid sulfonic acids from an aqueous extract of *Isatis indigotica* roots and their antiviral activity. *Acta Pharm Sin B* 2017;**7**:334–41.
39. Meng LJ, Guo QL, Xu CB, Zhu CG, Liu YF, Chen MH, et al. Diglycosidic indole alkaloid derivatives from an aqueous extract of *Isatis indigotica* roots. *J Asian Nat Prod Res* 2017;**19**:529–40.
40. Meng L, Guo Q, Liu Y, Shi J. 8,4′-Oxyneolignane glucosides from an aqueous extract of "ban lan gen" (*Isatis indigotica* root) and their absolute configurations. *Acta Pharm Sin B* 2017;**7**:638–46.
41. Meng LJ, Guo QL, Zhu CG, Xu CB, Shi JG. Isatindigodiphindoside, an alkaloid glycoside with a new diphenylpropylindole skeleton from the root of *Isatis indigotica*. *Chin Chem Lett* 2018;**29**:119–22.
42. Meng L, Guo Q, Chen M, Jiang J, Li Y, Shi J. Isatindolignanoside A, a glucosidic indole-lignan conjugate from an aqueous extract of the *Isatis indigotica* roots. *Chin Chem Lett* 2017http://dx.doi.org/10.1016/j.cclet.2017.12.001.
43. Jiang B, Lin S, Zhu C, Wang S, Wang Y, Chen M, et al. Diterpenoid alkaloids from the lateral root of *Aconitum carmichaelii*. *J Nat Prod* 2012;**75**:1145–59.
44. Jiang ZB, Jiang BY, Zhu CG, Guo QL, Peng Y, Wang XL, et al. Aromatic acid derivatives from the lateral roots of *Aconitum carmichaelii*. *J Asian Nat Prod Res* 2014;**16**:891–900.
45. Jiang ZB, Meng XH, Jiang BY, Zhu CG, Guo QL, Wang SJ, et al. Two 2-(quinonylcarboxamino)benzoates from the lateral roots of *Aconitum carmichaelii*. *Chin Chem Lett* 2015;**26**:653–6.
46. Meng XH, Jiang ZB, Zhu CG, Guo QL, Xu CB, Shi JG. Napelline-type C_{20}-diterpenoid alkaloid iminiums from an aqueous extract of "fu zi": solvent-/base-/acid-dependent transformation and equilibration between alcohol iminium and aza acetal forms. *Chin Chem Lett* 2016;**27**:993–1003.
47. Meng XH, Jiang ZB, Guo QL, Shi JG. A minor arcutine-type C_{20}-diterpenoid alkaloid iminium constituent of "fu zi". *Chin Chem Lett* 2017;**28**:588–92.
48. Meng XH, Guo QL, Zhu CG, Xu CB, Shi JG. Unprecedented C_{19}-diterpenoid alkaloid glycosides from an aqueous extract of "Fu Zi": neoline 14-*O*-L-arabinosides with four isomeric L-anabinosyls. *Chin Chem Lett* 2017;**28**:1705–10.
49. Guo QL, Xia H, Shi G, Zhang T, Shi J. Aconicarmisulfonine A, a sulfonated C_{20}-diterpenoid alkaloid from the lateral roots of *Aconitum carmichaelii*. *Org Lett* 2018;**20**:816–9.
50. Pelletier SW, Mody NV, Varughese KI. Szu-Ying C. Fuziline, a new alkaloid from the Chinese drug "Fuzi" (*Aconitum carmichae* Debx.). *Heterocycles* 1982;**18**:47–9.
51. Pelletier SW, Ying CS, Joshi BS, Desai HK. The structures of forestine and foresticine, two new C_{19}-diterpenoid alkaloids from *Aconitum forrestii* Stapf. *J Nat Prod* 1984;**47**:474–7.
52. Pelletier SW, Djarmati Z, Lajsic S, De Camp WH. Alkaloids of *Delphinium staphisagria*. The structure and stereochemistry of delphisine, neoline, chasmanine, and homochasmanine. *J Am Chem Soc* 1976;**98**:2617–25.
53. Pelletier SW, Djarmati Z. Carbon-13 nuclear magnetic resonance: aconitine-type diterpenoid alkaloids from *Aconitum* and *Delphinium* species. *J Am Chem Soc* 1976;**98**:2626–36.
54. Liu W, Gou XJ, Song Q, Chen FZ. Neoline from *Aconitum flavum* Hand. *Acta Crystallogr Sect E Struct Rep Online* 2011;**67**:o1435.
55. Ahmad H, Ahmad S, Khan E, Shahzad A, Ali M, Tahir MN, et al. Isolation, crystal structure determination and cholinesterase inhibitory potential of isotalatizidine hydrate from *Delphinium denudatum*. *Pharm Biol* 2017;**55**:680–6.
56. Wang FP, Chen QH. The C_{19}-diterpenoid alkaloids. In: Cordell GA, editor. *The alkaloids: chemistry and biology*. New York: Elsevier Science; 2010. p. 1–577.
57. Zhang ZT, Wang L, Chen QF, Chen QH, Chen DL, Liu XY, et al. Revisions of the diterpenoid alkaloids reported in a JNP paper (2012, 75, 1145–1159). *Tetrahedron* 2013;**69**:5859–66.
58. Wang FP, Chen DL, Deng HY, Chen QH, Liu XY, Jian XX. Further revisions on the diterpenoid alkaloids reported in a JNP paper (2012, 75, 1145–1159). *Tetrahedron* 2014;**70**:2582–90.
59. Levrier C, Sadowski MC, Nelson CC, Davis RA. Cytotoxic C_{20} diterpenoid alkaloids from the Australian endemic rainforest plant *Anopterus macleayanus*. *J Nat Prod* 2015;**78**:2908–16.
60. Chen Q. *Experimental methodology of pharmacology*. Beijing: People's Health Press; 742–70.